DEFORMATION BEHAVIOUR OF Cu-Zn-Al ALLOYS AND ITS EFFECT ON TRANSFORMATION HYSTERESIS①

Wang Mingpu, Xu Genyin*, Yin Zhiming
Department of Materials Science and Engineering, Central South University of Technolgy, Changsha 410083
* *Anhui Institute of Technology, Hefei 230069*

ABSTRACT The deformation behaviour of Cu-Zn-Al alloys and its effect on the transformation hysteresis were studied. It is shown that the critical stress for martensite boundary movement and the intrinsic transformation hysteresis of the alloys can be raised by increasing Al content and adding Mn element. For Cu-10. 2 Al-4. 9 Mn-4. 6 Zn-0. 3 Zr alloy, its transformation hysteresis increases more rapidly and its reversible martensite amount decreases more slowly as the strain increases. The main reason is that the increasing of Al content and adding of Mn element can strengthen the alloy and make the grains become more fine, which can improve the deformation resistance, reduce the irreversible defaults and make the energy for changing the martensite configuration increase. The wide transformation hysteresis effect of Cu-10. 2 Al-4. 9 Mn-4. 6 Zn-0. 3 Zr alloy were discussed as well, according to structure changes during deformation.

Key words shape memory alloy Cu-Zn-Al alloy martensite transformation boundary movement transformation hysteresis

1 INTRODUCTION

Cu-Zn-Al shape memory alloys (SMA) were studied by many authors[1-4] mainly on the alloys with Al content from 4% to 6%. But few studies were reported about the alloys whose Al contents are higher than 8% because of their poor workability. The wide transformation hysteresis (WTH) effect can be used for shape memory connector. So far, the investigation of the WTH effect has focused on Ni-Ti-Nb SMA and Fe-base SMA[5-8]. In this paper, the deformation behaviour of Cu-Zn-Al alloys and its effect on the transformation hysteresis were studied by increasing Al content and adding Mn element.

2 EXPERIMENTAL

The tested alloys were induction melted in graphite crucibles, cast into flat ingots, then hot-rolled into sheets of 1 mm thickness. The compositions of the alloys and their M_s temperatures, as well as their heat treatment conditions were listed in Table 1.

The tensile experiments were conducted on an Instron testing machine with specimens whose gauge sizes are 110 mm × 3 mm × 1 mm (for $\rho - t$ curve measurements) and 50 mm × 10 mm × 1 mm (for optical metalloscope and TEM observations). The optical microstructures were analysed on a Polyvar metalloscope with polarized light. The TEM specimens were mechanically thinned into 0. 2 mm thickness in 0 ℃ water, then electropolished into 0. 1 mm and finally jet electropolished with a solution of 30 HNO_3+70CH_3OH at −30∼−10 ℃. The TEM observations were carried out on a H-800 electron microscope operated at 200 kV.

Fig. 1 shows the definitions of the main martensite transformation parameters of the

① Received Nov. 17, 1994; accepted Jan. 23, 1995

Table 1 Compositions(%), M_s temperatures(℃) and heat treatment conditions of the alloys

Alloy No.	Zn	Al	Mn	Zr	Cu	M_s	Heat Treatment
1#	26.0	4.0	—	0.3	Remainder	35	Held at 850 ℃ for 5 min, quenched into room temperature water, then aged in boiling water for 30 min.
2#	21.3	5.9	—	0.3	Remainder	81	Held at 850 ℃ for 5 min, quenched into 140 ℃ oil and aged in it for 20 min.
3#	4.6	10.2	4.9	0.3	Remainder	37	Held at 850 ℃ for 5 min, air cooled, then aged in boiling water for 30 min.

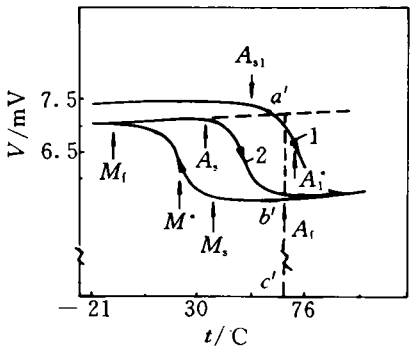

Fig. 1 $\rho - t$ curve of the deformed alloys on which the transformation temperatures, W_{TH} and R_M are defined

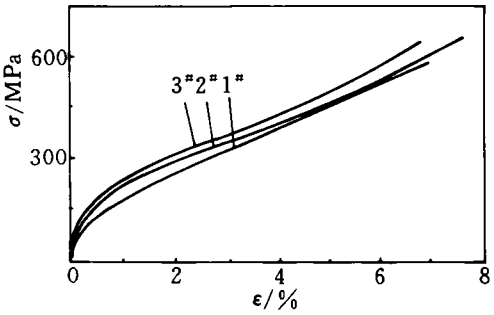

Fig. 2 $\sigma - \varepsilon$ curves of the alloys tested below M_s temperatures

deformed alloys, such as M_s, M_f, A_s, A_f, width of transformation hysteresis $W_{TH} = (A_1^* - M^*)$ and normalized reversible martensite amount $R_M = (a'b'/a'c')/(ab/ac)$, where (ab/ac) expresses the R_M of undeformed alloy which is supposed to be 100%.

3 RESULTS AND DISCUSSION

3.1 *Deformation and Its Effect on Martensite Transformation*

Fig. 2 shows the tensile curves of the experimental alloys tested at room temperature (below M_s). It can be seen that the contours of three curves are similar. But they move higher successively according to the sequence of the alloy number 1#, 2# and 3#. If $\sigma_{0.2}$ is defined as apparent "critical yield stress", it can be found that they increase successively, that is, 80, 110 and 128 MPa for alloy 1#, 2# and 3# respectively.

Fig. 3 shows the relations between the W_{TH} (Fig. 3a), the R_M (Fig. 3b) and the tensile strain ε of three alloys respectively. It can be seen that the intrinsic transformation hysteresis of the undeformed alloys increases in sequence of alloy 1#, 2# and 3#. For all experimental alloys, the increase of the W_{TH} and the decrease of the R_M conform the similar rule as the deformation increases. But for alloys 3#, the W_{TH} increases more rapidly and the R_M declines more slowly than the others. For example, when $\varepsilon = 5\%$, the $(A_1^* - M^*)$ of alloy 3# is larger than 90 ℃, whereas those of alloy 1# ad 2# only reach 60 and 54 ℃ respectively. Moreover, the R_M of alloy 3# can reach 90% approximately at that time, whereas

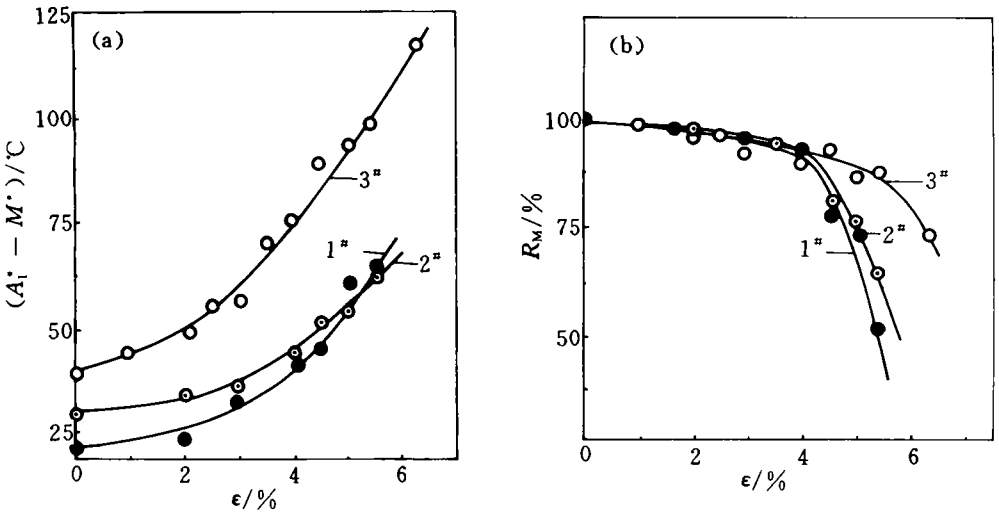

Fig. 3 Relations between (a)—the transformation hysteresis ($A_1^* - M^*$), (b)—the reversible martensite amount (R_M) and the strain ε of the experimental alloys

those of the two other alloys have been declining dramatically.

For alloy 3#, the higher R_M means the larger SME. The main reason may be the Al increasing and Mn adding in the alloy, which can strengthen the alloy and improve the deformation resistance[9, 10], so the irreversible defaults caused by plastic slip can be reduced to some extent. The intrinsic transformation hysteresis is a reflection of moving ability of the martensite boundaries under thermal activation, whereas the apparent "critical yield stress" is a measurement for martensite boundaries to start moving under tensile. For alloy 3#, both intrinsic transformation hysteresis and apparent "critical yield stress" are larger, which implies more difficult to move martensite boundaries. This may be related with the alloy strengthening. On the other hand, more fine grains can be obtained by combined adding Mn and Zr in the alloy. The strain caused by movement of martensite boundaries may be restricted near the grain boundaries, which makes the martensite boundaries difficult to move.

3. 2 *Structure Changes of Deformed Alloy* 3#

The structure changes during deformation were studied by many authors for alloys similar to alloy 1# and 2#. Mainly, the structure changes of the deformed alloy 3# were discussed in this paper. Fig. 4 shows the optical microstructures of alloy 3# subjected to different deformation. Mainly, the undeformed structure is the martensites whose morphologies are self-accomodating spear like variants and many parallel variants (Fig. 4a). In addition, convex lens like variants can be seen somewhere which haven't been reported in Cu-Zn-Al alloys with Al content from 4% to 6%. We guess that these convex lens like variants may possess twin substructure because there are many fine streaks on them. A large amount of observations show that the degree of deformation is significantly different from one grain to another as observed by Adachi *et al*[11]. So it may be the common characteristics of the polycrystalline alloy. The white acicular streaks shown in Fig. 4b may result from stress-induced 2*H* transformation. The obvious preferential growth of

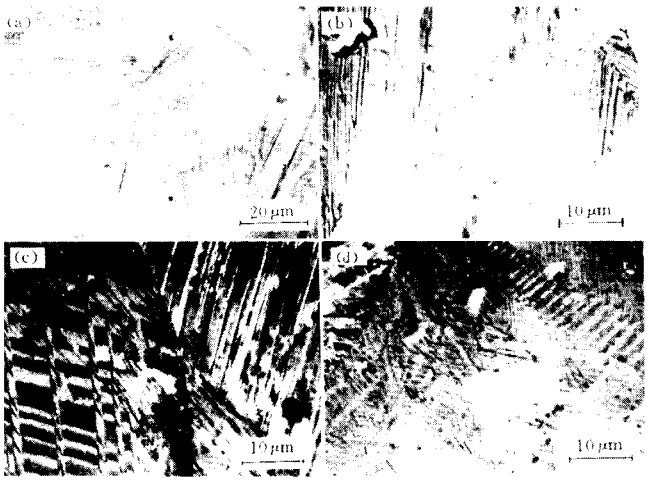

Fig. 4 Optical microstructures of the deformed Cu-10. 2 Al-4. 9 Mn-4. 6 Zn-0. 3 Zr alloy
(a)— $\varepsilon=0$; (b)— $\varepsilon=2\%$; (c)— $\varepsilon=4\%$; (d)— $\varepsilon=5\%$

the variant is shown in Fig. 4c, where it can be seen that a variant group has almost coalesced into a main variant. On the left of Fig. 4c, it can be seen that the shear deformation of host variants can be caused by projecting new variants in them, through which the cross structures are formed. These strutures were observed in stress-induced $\beta_1 \rightarrow M$ transformation by Deleay *et al*[3], but they were formed here obviously by cutting between new variants and the host variants. Fig. 4d shows the "band structure" formed in single variant at higher strain. These band structures grow along the basic plane of the host variants and may come from the $18R \rightarrow 2H$ transformation[11].

Fig. 5 shows the TEM morphologies and related electron diffraction patterns of alloy 3#. A large amount of observations reveal that the main structure of undeformed alloy is faulted $18R$ martensite (Fig. 5a). In addition, there exists a few twined martensite, such as convex lens like martensite (Fig. 4a). Under deformation, the martensite structure changes gradually from $18R$ to $2H$. Fig. 5b and Fig. 5c show the two kinds of $2H$ twined martensites which exist in deformed alloy, i. e, $(101)_{2H}$ twin and $(121)_{2H}$ twin. In the $(101)_{2H}$ twin, there exists high density stacking faults along the basic planes of the twin variants, which produce the diffraction streaks along $[001]_{2H}$ direction in related diffraction pattern. The existing of faults means that the $2H$ martensite may form through a shear along $\langle 100\rangle_{18R}$ direction on $(001)_{18R}$ basic plane of $18R$ martensite. In some area of twin variants, no fault can be found, such as down left corner of Fig. 5b. This may be due to further shear deformation of the variants. In addtion, the angle between $[001]_{2H}$ and $[100]_{2H}$ is 90°, which means that the stress-induced martensite from $18R$ structure is $N2H$ one. Fig. 5c illustrates

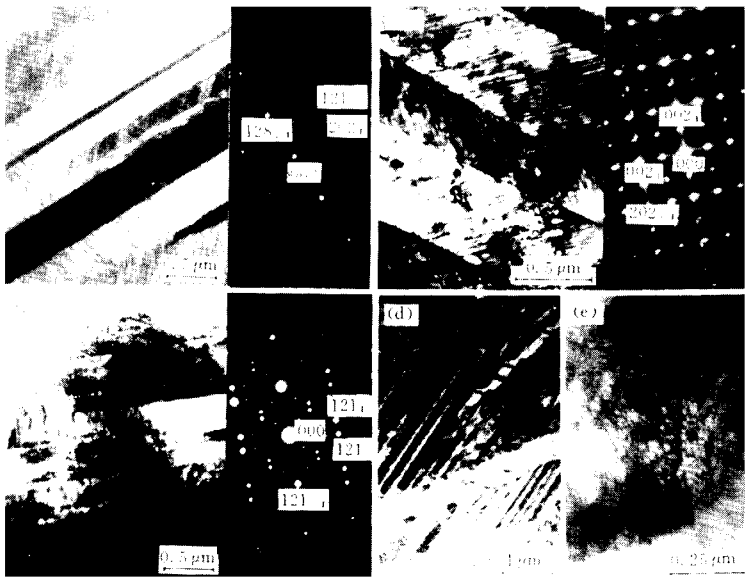

Fig. 5 TEM morphologies and related electron diffraction patterns of the deformed Cu-10.2 Al-4.9 Mn-4.6 Zn-0.3 Zr alloy

(a)— $\varepsilon = 0$, $(\overline{1}28)_{18R}$ twin; (b)— $\varepsilon = 2\%$, $(101)_{2H}$ twin; (c)— $\varepsilon = 5\%$, $(\overline{1}21)_{2H}$ twin; (d)— $\varepsilon = 5\%$, serrated interfaces and twin debris; (e) $\varepsilon = 5\%$, tangled dislocations in the martensites and on the variant boundaries

the twin morphology of stress-induced $2H$ martensite whose ends are projected into the interfaces of the host variants, making them become serrated ones. In some regions, the twin plates are broken into debris.

The W_{TH} effect may be mainly caused by two reasons. First, the coalescence of variants, cross structures, band structures, serrated boundaries and twin debris, all these structures caused by deformation make the coherent bounderies between the host variants destroyed to some extent. These structure changes make the martensite become more stable and difficult to reverse. Second, the stress-induced $2H$ martensites are normal ones. This means that the deformation can change the atom configuration. Similar to the martensite stabilization phenomenon caused by thermal activation[12-14], it makes the martensite more difficult to reverse and results in the W_{TH} effect. In some regions, such as the variant cross regions and the intervariant boundaries, the tangled dislocations can be seen under higher strain(Fig. 5c), which not only impedes the martensite to reverse and cause the W_{TH} effect, but also make the martensites lose their thermoelasticity and result in decrease of the R_M.

4 CONCLUSIONS

(1) Increasing Al and adding Mn in Cu-Zn-Al alloys can strengthen the alloys, make the grains finer, which results in increasing of critical stress for moving martensite boundaries, as well as increasing of the intrinsic transformation hysteresis.

(2) The W_{TH} effect can be induced in Cu-Zn-Al alloys by deformation below M_s temperature. For Cu-10.2 Al-4.9 Mn-4.6 Zn-0.3 Zr alloy, its W_{TH} increases more rapidly and its R_M decreases more slowly with the increasing of strain, which may be related with the strengthening of the alloy and the reducing of the irreversible defaults.

(3) For Cu-10.2 Al-4.9 Mn-4.6 Zn-0.3 Zr alloy, new structures of the martensites can be induced by deformation, such as the coalescence of variants, cross structures, band structures, serrated boundaries, twin debris, tangled dislocations and $18R \rightarrow 2H$ transformation. These movements destroy the coherent boundaries of the martensites and change the atom configuration, which results in the W_{TH} effect.

REFERENCES

1 Chu Youyi, Hsu T Y, Ko T. Shape Memory Alloy '86, Proc of the Int Symp on SMA, Guilin, China. Beijing: China Acad Publ, 1986: 201—349.
2 Chu Youyi, Tu Hailing. Shape Memory Materials '94, Proc of the Int Symp on SMM, Beijing, China. Beijing: Int Acad Publ, 1994: 309—437.
3 Delaey L *et al*. In: Perkins J ed, Shape Memory Effect in Alloys, New York: Plenum Press, 1975: 351.
4 Wayman C M. In: Perkins J ed, Shape Memory Effect in Alloys, New York: Plenum Press, 1975: 1.
5 During T W. Mater Sci Forum, 1990, (56—58): 679.
6 Zhang Chunsheng, Cai Wei, Zhao Liancheng. Acta Metall Sinica, 1991, 3A: 211.
7 Yuan Guansheng. In: Conf on SMA of China, Beijing, 1988.
8 Wang Xiaoxiang, Zhao Liancheng. In: Conf on Martensite transformation, Qinhuangdao, 1990: 2, 275.
9 Melton K N, Mercier O. Metall Trans, 1979, 10A: 875.
10 Lu Qiqing *et al*. J of Functional Materials, 1993, 24(2): 162.
11 Adachi K, Perkings J. Metall Trans, 1986, 17A: 945.
12 Humbeeck J V *et al*. Script Metall, 1984, 18: 893.
13 Scarsbrook G, Cook J M, Stoblos W M. Metall Trans, 1984, 15A: 1977.
14 Wang Mingpu, Liu Jinwen. Acta Metall Sinica, 1990, 3 (6A): 439.

(Edited by Peng Chaoqun)